Generation of two-color continuous variable quantum entanglement at 0.8 and 1.5 μm

Yongmin Li,[a)] Xiaomin Guo, Zengliang Bai, and Chunchun Liu
State Key Laboratory of Quantum Optics and Quantum Optics Devices, Institute of Opto-Electronics, Shanxi University, Taiyuan 030006, People's Republic of China

(Received 28 April 2010; accepted 30 June 2010; published online 20 July 2010)

Two-color continuous variable quantum entanglement at 0.8 and 1.5 μm was experimentally demonstrated by using an above-threshold optical parametric oscillator based on a periodically poled $KTiOPO_4$ crystal. The system presented here has potential applications in future quantum information networks, e.g., it can be used to made a connection between a quantum memory device based on alkaline atoms and a quantum communication device based on telecommunication optical fibers. © *2010 American Institute of Physics*. [doi:10.1063/1.3467045]

Quantum entangled states are the fundamental resources of quantum communication and quantum information processing. Alkaline atoms that absorb and emit at wavelengths around 0.8 μm have been employed to store the optical quantum states.[1,2] The presence of telecommunication low-loss optical fibers make the wavelength of 1.5 μm suitable for distribution of optical quantum states over long distances.[3] In future quantum information network, systems of different nature need to be linked together. Two-color quantum entangled states at 0.8 and 1.5 μm are of interest for long-distance quantum information processing,[4,5] for example, it can be utilized to make a connection between a quantum memory device based on alkaline atoms and a quantum communication device based on telecommunication optical fibers. Polarization-entangled photons at 0.8 and 1.6 μm have been generated in quasi-phase-matched two-crystal and single-crystal sources.[6–8] By using above-threshold nondegenerate optical parametric oscillator (NOPO), two-color and three-color continuous variable (cv) entangled states have been prepared.[9–11] Entanglement of fundamental and second-harmonic fields was also observed in a depleted optical parametric amplifier.[12] In this letter, two-color cv entangled beams at 0.8 and 1.5 μm were generated experimentally by using an above-threshold NOPO. Amplitude quadrature difference correlation of 1.2 dB and phase quadrature sum correlation of 0.7 dB were observed. The entanglement was verified according to the inseparability criterion.[13]

The schematic diagram of our experimental setup is shown in Fig. 1. The laser source is a frequency-doubled neodymium-doped yttrium lithium fluoride (Nd:YLF) single-frequency continuous wave laser at 526.5 nm. A Faraday isolator was set in the input light of the NOPO to eliminate the back reflection. The NOPO cavity[14] consists of two planoconcave mirrors with 30 mm radii of curvature and the beam waist of the resonator is about 50 μm inside the nonlinear crystal. The input coupler was coated for high reflectivity at 0.8 and 1.5 μm and high transmission at 526.5 nm. The output coupler was coated for high reflectivity at 526.5 nm and partial transmission (about 3%) at 0.8 and 1.5 μm. A 20 mm long periodically poled $KTiOPO_4$ crystal (PPKTP) was chosen as the nonlinear crystal for its relatively high nonlinear coefficient and room temperature operation. Both end faces of the PPKTP crystal were antireflection coated at 526.5 nm, 0.8, and 1.5 μm. The crystal was put in a temperature-controlled oven with accuracy of 0.01 °C. In our current experiment, the temperature of the crystal oven was set to 15 °C and the measured wavelengths of the signal and idler beams were 806 nm and 1518 nm, respectively. The corresponding threshold power of the NOPO was 11.6 mW.

To observe the quantum entanglement, the NOPO cavity was actively controlled to maintain resonance with the down-converted light fields. The generated signal and idler beams were separated by a dichroic beam splitter and each directed to a single-ended analysis cavity (A1 and A2). Here the analysis cavities were used to investigate the phase noise properties of the signal/idler field,[15,16] because it was shown that for analysis frequencies larger than $\sqrt{2}\delta f_{ac}$, the phase fluctuations of the incident optical field can be completely converted into amplitude fluctuations of the reflected optical field when $\Delta \approx \pm \delta f_{ac}/2$, here δf_{ac} is the bandwidth of the analysis cavity (full width half maximum) and Δ is detuning between the incident field central frequency and the analysis cavity resonance frequency. In our experiment, two three-mirror ring cavities with bandwidth of 6.25 MHz were utilized as shown in Fig. 1. Each reflected signal/idler optical field from the analysis cavity was directed to a homodyne detection system, which were built from two ETX-500 (Epitaxx) and two FND-100Q (EG&G) photodiodes, respec-

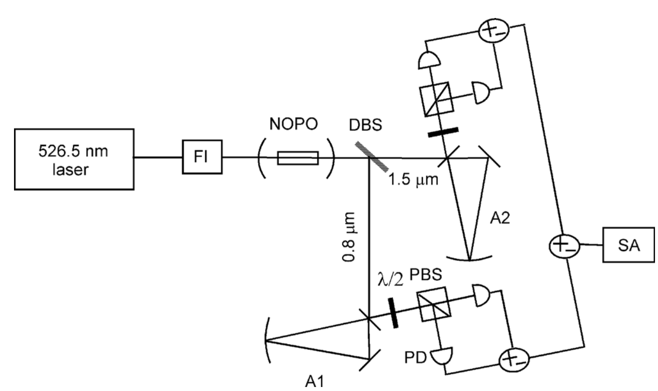

FIG. 1. Schematic diagram of the experimental setup. FI, Faraday isolator; DBS, dichroic beam splitter; PD, photodetectors; PBS, polarizing beam splitter; SA, spectrum analyzer; and A1, A2, analysis cavity.

[a)]Electronic mail: yongmin@sxu.edu.cn.

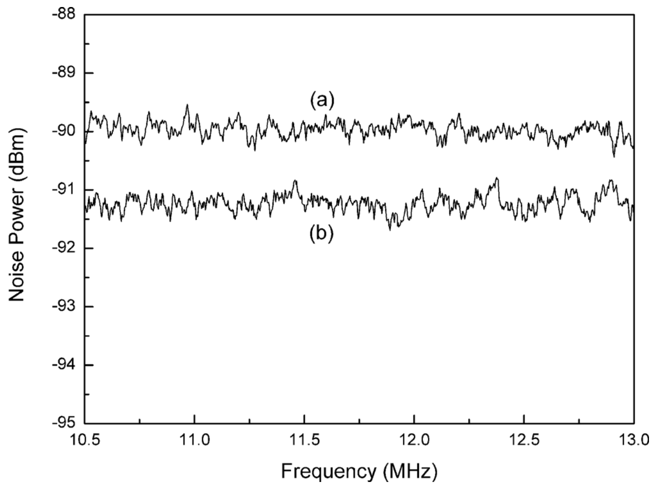

FIG. 2. Measured amplitude quatrature difference noise spectrum between the 0.8 and 1.5 μm optical fields. (a) Quantum noise limit. (b) Amplitude quadrature difference noise spectra. The settings of the spectrum analyzer: resolution bandwidth is 75 kHz and video bandwidth is 10 Hz.

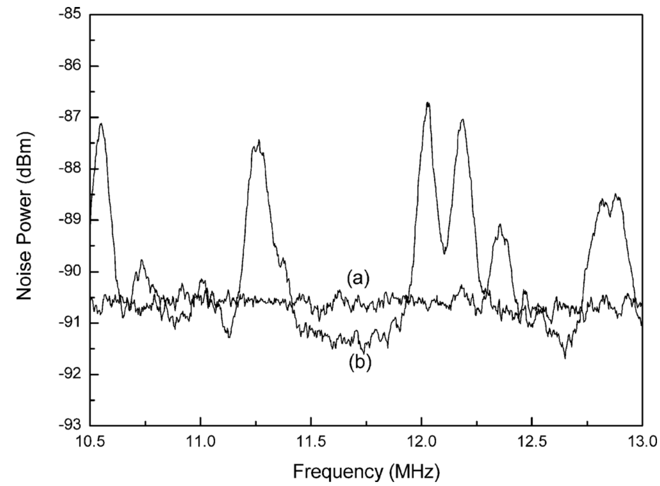

FIG. 3. Measured phase quadrature sum noise spectrum between the 0.8 and 1.5 μm optical fields. (a) Quantum noise limit. (b) Phase quadrature sum noise spectra. The settings of the spectrum analyzer are same with those of Fig. 2.

tively. A half-wave plate in front of a polarizing beam splitter acts as a 50/50 beam splitter. The photocurrent signals were recorded using a spectrum analyzer. For each beam (signal/idler), the noise power of the difference photocurrent signal corresponds to the quantum noise limit (QNL), and the noise power of the sum photocurrent signal corresponds to the amplitude quadrature noise power. When both analysis cavities are far detuned ($\Delta \gg \delta f_{\mathrm{ac}}$), no conversion was occurred between the quadratures of the incident optical field and those of the reflected optical field, so the difference of the sum (difference) photocurrent signal of each beam corresponds to the amplitude quadrature difference noise power (the combined QNL) of the twin beams. When both analysis cavities are locked on half maximum of the resonance peak ($\Delta \approx \pm \delta f_{\mathrm{ac}}/2$), because of the conversion of the quadrature fluctuation between the incident optical field and reflected optical field, the sum of the sum (difference) photocurrent signal of each beam corresponds to the phase quadrature sum noise power (the combined QNL) of the twin beams.

At pump power of 15 mW, both the amplitude quadrature and phase quadrature correlations were measured using the method mentioned above. Figure 2 is the measured amplitude quadrature difference noise spectrum between the 0.8 μm signal and 1.5 μm idler fields from 10.5 MHz to 13 MHz. 1.2 dB of amplitude quadrature difference quantum correlation was observed at 11.7 MHz. Figure 3 is the measured phase quadrature sum noise spectrum. The observed phase quadrature sum quantum correlation was 0.7 dB at 11.7 MHz. In Figs. 2 and 3, the electronic dark noise of the detectors which is 4.5 dB below the QNL has been subtracted. The quantum entanglement between the 0.8 μm signal and 1.5 μm idler optical fields was verified according to the inseparability criterion[13] $\langle\Delta^2(X_1 - X_2)\rangle + \langle\Delta^2(Y_1 + Y_2)\rangle = 1.61 < 2$, here X_j and $Y_j (j=1,2)$ are amplitude and phase quadratures. As shown in Fig. 3, there are some narrow peaks which are about 4 dB above the noise floor in the phase quadrature sum noise spectra. We hypothesized that these peaks came from the phenomenon of guided acoustic wave Brillouin scattering (GAWBS).[12,17,18] First, we checked the individual noise spectra of signal/idler beam and it was found there exist similar noise peaks in the phase quadrature noise spectra but the noise peaks were absent in the amplitude quadrature. This is consistent with the prediction of GAWBS. Second, we measured the additional phase noise of 1.5 μm idler beam as a function of its output power and it is shown that the additional phase noise (normalized to QNL) increases linearly with the idler power (Fig. 4). It is noted that similar phenomena were also observed in Ref. 18. At last, the additional phase noise consists of many peaks; we attribute this to the guided acoustic modes (phonons).

The amplitude/phase quadrature correlation noise spectrum from a NOPO above threshold can be given by[19]

$$R_a(f) = 1 - \eta_D \eta_{OC} \frac{1}{1 + (f/f_c)^2}, \tag{1}$$

$$R_p(f) = 1 - \eta_D \eta_{OC} \frac{1}{\sigma^2 + (f/f_c)^2}, \tag{2}$$

where $R_a(f)$ $[R_p(f)]$ is amplitude (phase) quadrature correlation noise spectrum (normalized to the QNL), η_D is the de-

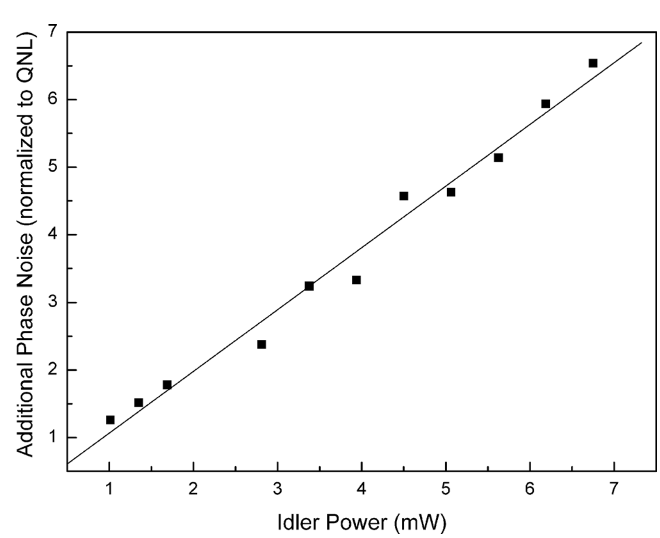

FIG. 4. Measured additional phase noise power as a function of idler power at 11.2 MHz. Solid squares are the experimental results and solid curve is a linear fitting.

tection efficiency, η_{OC} is the escape efficiency, f_c is the bandwidth of the NOPO cavity, $\sigma=\sqrt{P/P_{th}}$ is the pump parameter (P is the pump power and P_{th} is the threshold power of the NOPO). By using the following experimental parameters: $\eta_D=0.63$, $\eta_{OC}=0.76$, $f_c=12$ MHz, $f=11.7$ MHz, and $\sigma=\sqrt{1.3}$, the theoretical prediction from Eqs. (1) and (2) are $R_a(f)=0.75$ and $R_p(f)=0.79$, and the corresponding values in decibel units are 1.2 and 1.0 dB. The theoretical value of $R_a(f)$ is in good agreement with the experimental value of 1.2 dB, while it is not the case for the phase quadrature correlation. The possible reason for such discrepancy is the influence of the excess noises including the excess phase noise of pump laser and the potential GAWBS noise.

The theoretical simulation suggests that the nonperfect detection efficiency (including the quantum efficiency of the photodiode and the optical propagation efficiency) and the escape efficiency were the main limitations in our current experiment. These can be partially overcome by using high quality optical elements with better coatings to reduce greatly unwanted linear losses. For the excess noises, a filter cavity can be built to suppress the excess phase noise of the pump laser. It is noted from Eq. (2) that the quantum correlation in the phase quadrature sum improves as the pump power approaches the threshold, at the same time the reduced pump power will lead to lower down-conversion power that is preferred for the suppressing of the potential GAWBS noise. In our current experiment, the NOPO can only be operated above 1.3 times threshold because of the output stability. By improving the stability of the pump laser and the NOPO cavity length, etc., it is possible to operate the NOPO at lower pump power.

In conclusion, two-color cv quantum entanglement at 0.8 and 1.5 μm was experimentally demonstrated by using an above-threshold NOPO based on PPKTP crystal. The quantum entanglement was verified according to the inseparability criterion. The source presented here has potential applications in future quantum information networks, such as transfer of the cv quantum information between alkaline atoms and light fields of telecommunication wavelength.

This research is supported by the National Science Foundation of China (Grant No. 60608011), the Research Fund for the Doctoral Program of Higher Education (Grant No. 20060108005), the TYAL, the National Key Basic Research Program of China (Grant No. 2010CB923101), the NSFC Project for Excellent Research Team (Grant No. 60821004).

[1] J. Appel, E. Figueroa, D. Korystov, M. Lobino, and A. I. Lvovsky, Phys. Rev. Lett. **100**, 093602 (2008).
[2] K. Honda, D. Akamatsu, M. Arikawa, Y. Yokoi, K. Akiba, S. Nagatsuka, T. Tanimura, A. Furusawa, and M. Kozuma, Phys. Rev. Lett. **100**, 093601 (2008).
[3] D. Stucki, N. Walenta, F. Vannel, R. T. Thew, N. Gisin, H. Zbinden, S. Gray, C. R. Towery, and S. Ten, New J. Phys. **11**, 075003 (2009).
[4] J. H. Shapiro, New J. Phys. **4**, 47.1 (2002).
[5] S. Lloyd, M. S. Shahriar, and J. H. Shapiro, Phys. Rev. Lett. **87**, 167903 (2001).
[6] E. J. Mason, M. A. Albota, F. König, and F. N. C. Wong, Opt. Lett. **27**, 2115 (2002).
[7] D. Ljunggren, M. Tengner, P. Marsden, and M. Pelton, Phys. Rev. A **73**, 032326 (2006).
[8] S. Sauge, M. Swillo, M. Tengner, and A. Karlsson, Opt. Express **16**, 9701 (2008).
[9] A. S. Villar, L. S. Cruz, K. N. Cassemiro, M. Martinelli, and P. Nussenzveig, Phys. Rev. Lett. **95**, 243603 (2005).
[10] X. L. Su, A. H. Tan, X. J. Jia, Q. Pan, C. D. Xie, and K. C. Peng, Opt. Lett. **31**, 1133 (2006).
[11] A. S. Coelho, F. A. S. Barbosa, K. N. Cassemiro, A. S. Villar, M. Martinelli, and P. Nussenzveig, Science **326**, 823 (2009).
[12] N. B. Grosse, S. Assad, M. Mehmet, R. Schnabel, T. Symul, and P. K. Lam, Phys. Rev. Lett. **100**, 243601 (2008).
[13] L. M. Duan, G. Giedke, J. I. Cirac, and P. Zoller, Phys. Rev. Lett. **84**, 2722 (2000).
[14] Y. M. Li, X. M. Guo, X. Y. Wang, and K. S. Zhang, J. Opt. Soc. Am. B **27**, 842 (2010).
[15] P. Galatola, L. A. Lugiato, M. G. Porreca, P. Tombesi, and G. Leuchs, Opt. Commun. **85**, 95 (1991).
[16] A. S. Villar, M. Martinelli, and P. Nussenzveig, Opt. Commun. **242**, 551 (2004).
[17] R. M. Shelby, M. D. Levenson, and P. W. Bayer, Phys. Rev. Lett. **54**, 939 (1985).
[18] J. E. S. César, A. S. Coelho, K. N. Cassemiro, A. S. Villar, M. Lassen, P. Nussenzveig, and M. Martinelli, Phys. Rev. A **79**, 063816 (2009).
[19] C. Fabre, E. Giacobino, A. Heidmann, and S. Reynaud, J. Phys. (Paris) **50**, 1209 (1989).